Significant Impact of Environment Stiffness and Joint Proximity on Sensory Integration of Position and Force Feedback

Master's Thesis

A.G.L. Engelen

Delft University of Technology

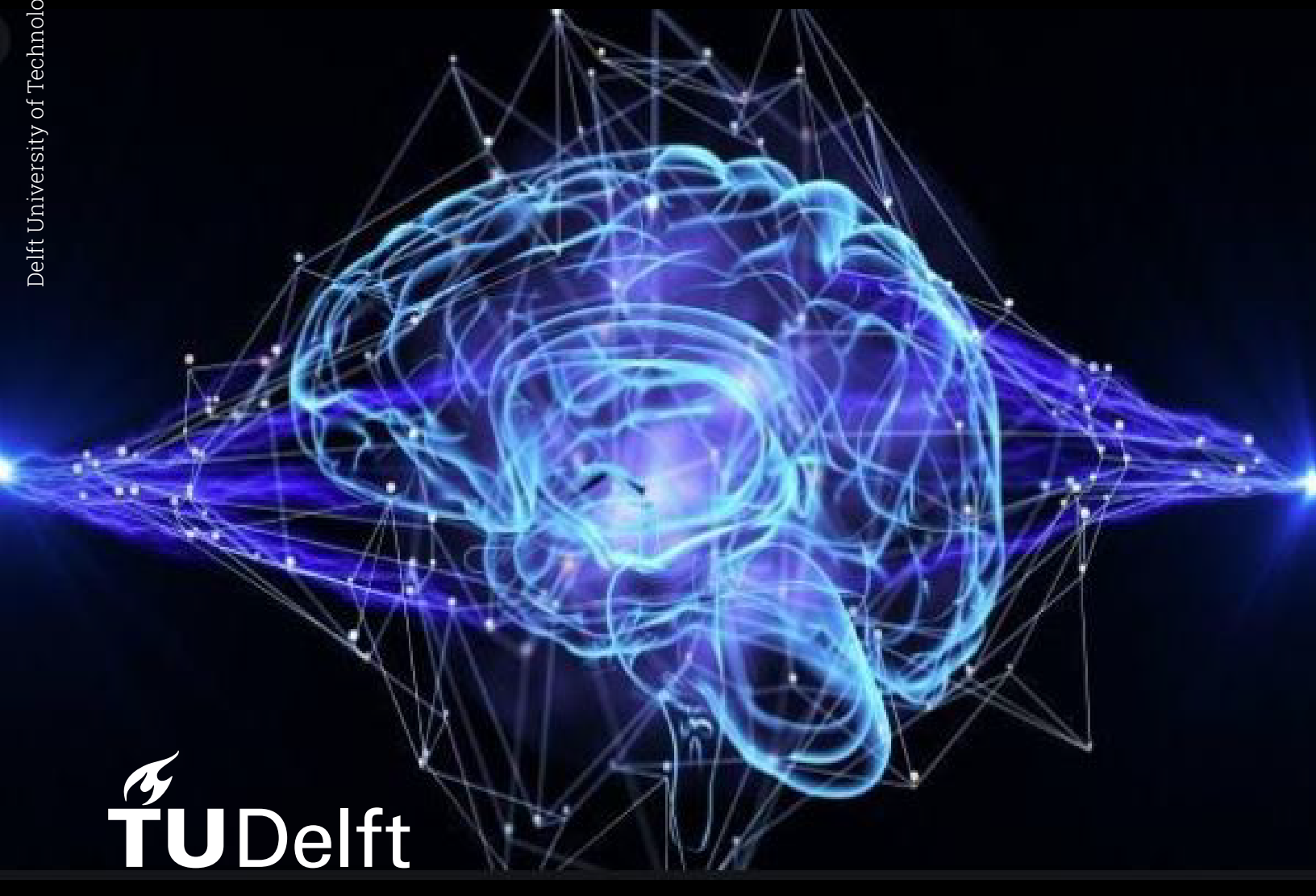

TU Delft

Significant Impact of Environment Stiffness and Joint Proximity on Sensory Integration of Position and Force Feedback

by

A.G.L. Engelen

(4869397)

Instructor:	Dr. ir. W. Mugge
Committee Members:	Dr. ir. W. Mugge (chair)
	Dr. ir. D.M. Pool (member)
Project Duration:	Mar., 2023 - Okt., 2023
Institution:	Delft University of Technology
Faculty:	Faculty of Mechanical, Maritime and Materials Engineering (3mE), Delft
Laboratory:	NeuroMuscular Control lab (NMClab)
Degree:	Master of Science in Mechanical Engineering
Presentation and Defense:	27 Okt 2023, 10:45 - 12:45

TU Delft

Significant Impact of Environment Stiffness and Joint Proximity on Sensory Integration of Position and Force Feedback

A.G.L. Engelen, 4869397
Supervisor: Dr. ir. W. Mugge

During human motor control, sensory information is integrated, and the influence of each cue depends on its variance. Sensory weighting within the proprioceptive system, specifically between force and position feedback, including its stiffness dependency, has been demonstrated for the shoulder and digits. Both studies encompass upper limb joints, but the impact of joint proximity on sensory integration remains unknown. In this study, we analyzed isolated vertical reaching movements of the wrist (palmar flexion), elbow (flexion), and shoulder (retroflexion) using a haptic robotic manipulator. We varied the stiffness constant of a virtual spring (15 N/rad, 50 N/rad, 80 N/rad) to assess the influence of environment stiffness on participants' ability to blindly reproduce a target force. A nonlinear spring was introduced to reveal the weighting strategy between force and position feedback. Differences in force and position when participants unknowingly operated in the nonlinear environment, compared to the linear environment, allowed us to calculate the weights of both feedback cues. Repeating the experiment for the three joints allowed us to assess the influence of joint location on the weighting strategy between force and position feedback. Ten participants performed a total of 720 reaches, covering three different stiffness conditions, three distinct joints, and ten separate runs, each consisting of eight reaches. We hypothesized that both environment stiffness and joint location have a significant impact on the weighting strategy. We expanded on existing findings that show a tendency toward up-weighting force feedback in the integration process as environment stiffness increases. Additionally, we examined whether force or position feedback is favored when the joint is more proximal. The hypothesis is supported by experimental evidence, as both stiffness and joint type revealed statistically significant effects on the weighting strategy ($p < 0.001$, $p = 0.020$, respectively). As environment stiffness increased, a shift from higher position weighting factors to higher force weighting factors was observed for all three joints. When comparing our findings to the Maximum Likelihood Estimation model predictions, we observed that the more proximal joints exhibited higher force weighting factors. Additionally, normalizing the experimental environment stiffness conditions over the maximal voluntary force of each joint times the moment arm and over the joint stiffness showed a similar trend. More distal joints, on the other hand, favored higher position weighting factors.

TU Delft Faculty of Mechanical, Maritime and Materials Engineering, Delft University of Technology, Delft, The Netherlands
A.G.L.Engelen@student.tudelft.nl

Introduction

Human motor control refers to the process in which the human nervous system coordinates movements of the body, involving the integration of sensory information. It is an adaptive process that varies depending on the environment in which we operate (Körding & Wolpert, 2004, 2006; Pasma et al., 2012; Rosenbaum, 2009). Our strategy to control our movements is influenced by the surroundings, and our brain seamlessly adjusts to the changing conditions to optimize performance. When you hop on a bicycle to go for a ride, you receive information from your senses, including visual feedback from your eyes and proprioceptive feedback from your muscles. Your brain uses this information to maintain balance and stability on the bike. The influence of each sensory information cue in the integration process depends on the variance of that particular cue, referred to as sensory weighting (Block & Bastian, 2011). Sensory weighting allows you to adapt your motor control effectively based on the information provided by your senses. Having a clear sight on the bike increases the influence of visual feedback, resulting in an increased weight assigned to visual feedback within the integration process. Proprioception allows us to perceive the position and movement of our body parts without relying on visual cues (Hoffman & Gregory Payne, 1995), and is therefore crucial for human motor control tasks. Proprioception contains position and force feedback, originating from our muscles (Mackinnon, 2018). Both sensory systems provide our brain with information which is integrated to formulate a comprehensive understanding of the body's posture and movement.

Extensive literature is available showing that the integration of sensory information during human motor control

tasks follows Bayesian integration, also referred to as sensorimotor integration (Körding & Wolpert, 2004, 2006; Saidi et al., 2012). These findings demonstrate that human motion is arranged through the integration of sensory input, accompanied by ongoing adjustments to the influence of various feedback cues, all aimed at optimizing motor output to minimize the variance. They present that all sensory cues influence the final estimate, but the degree of influence of each sensory cue in the process varies depending on its variance, which is referred to as the likelihood of each sensory cue. Incorporating pre-existing task-related beliefs, the sensory feedback is merged.

In many motor control tasks however, humans will rather have to combine multiple pieces of information instead of combining prior knowledge with the likelihood of sensory feedback cues, particularly when dealing with unfamiliar tasks (Lee et al., 2019). Consider the action of reaching for an object on a high shelf. Your brain quickly processes visual information to detect the object, simultaneously calculating the distance, height, and angle needed to reach it. It also considers the size and weight as we feel the object, anticipating the force required for a successful grasp. Both senses (vision and touch) provide our brain with information about the object, even if this information is uncertain. In literature, this process is referred to as cue combination (Alais & Burr, 2019). The computational challenge of integrating information from two sources is analogous to the manner in which we combine our prior beliefs with the likelihood of sensory input from a single cue, adhering to the principles of Bayesian integration.

One model that successfully predicts the optimal integration of the sensory signals based on the relative uncertainty, indicated by their variance is the Maximum Likelihood Estimation (MLE) (Landy et al., 1995; Ernst & Banks, 2002). The final estimate is a weighted average of the estimates derived from the individual cues, where the final estimate has a lower variance compared to the individual cues. The weights are defined as the relative reliability on the information obtained from the senses. Recall the example of grasping an object from the shelf. When an object is placed at a height that obstructs your line of sight, the reliability of information obtained from your visual system diminishes compared to situations where both the object and your hand are clearly visible. The weight attributed to the single cue estimate (in this case the visual information) reduces towards zero. The influence of the visual information cue within the integration process decreases, yet it will persist once the observation is made at any point during the movement (J Smeets et al., 2006).

Sensory integration within the same sensory modality also follows Bayesian integration. Van Beek et al. (2016) provided evidence for the haptic modality. Mugge et al. (2009) and Geelen et al. (2023) for the proprioceptive modality. Within the proprioceptive modality the two so called sub-modalities (force and position) are integrated following Bayesian integration rules. In different environments, the accuracy of the proprioceptive sub-modalities, position and force, play an important role in determining how well we can execute tasks and interact with our surroundings.

Extensive research exists in the field of human motor control, focusing on Bayesian integration, which involves the integration of proprioception with various sensory information types, as well as integrating the sub-modalities of proprioception. Based on the methodology, we can discern two prominent categories of experiments: reaching movements and balance control. These studies demonstrate that humans proficiently engage in Bayesian integration to process sensory information. This process entails filtering out less reliable data and adapting flexibly to environmental or task-related variations. Arguably, the presence of robotic devices in laboratory settings has led to an emphasis on upper extremities during reaching movement studies, whereas lower extremities take precedence in balance control investigations. Consequently, only a limited range of real-world context experiments exist, covering only a narrow range of joints. This raises questions regarding the influence of joint location on sensory integration. Given that sensory weighting is influenced by a range of factors including environmental conditions, task requirements, attention, prior beliefs, effort, and considering its asymmetric nature, the current investigations into the influence of joint location face limitations.

In stiffer environments, humans tend to prioritize force feedback over position feedback in comparison to less stiff environments. This is shown for the shoulder (Mugge et al., 2009), and the digits (Geelen et al., 2023). Both studies contain upper body joints, with one more distal, and the other more proximal. It is important to highlight that discernible differences exist between proximal and distal joints. As per definition, proximal joints have shorter ascending pathways, resulting in faster sensory information integration in the brain (Fei Yam et al., 2018). Another noteworthy aspect is that proximal joints exhibit a higher density of proprioceptors (Proske & Gandevia, 2012), implying a more accurate proprioceptive estimation for these joints. Additionally, distal joints possess distinct representations in the motor cortex compared to proximal joints (Hudson et al., 2017; Hatsopoulos et al., 2010), which could potentially in-

fluence the integration process. Moreover, there is a general consensus that proximal joints, such as the shoulder and hip, typically exhibit greater stiffness compared to distal joints like the wrist and ankle, possibly attributed to the engagement of distinct muscle groups. Also, proximal joints exhibit higher impedance, allowing for superior neural noise filtering compared to distal joints (Salmond et al., 2017). These differences suggest the potential presence of distinct proprioceptive strategies and receptors. However, these insights do not lead to a conclusive understanding of how these differences impact the integration of proprioceptive sub-modalities during human motor control tasks. Notwithstanding these distinctions between proximal and distal joints, both Mugge et al. (2009) and Geelen et al. (2023) provide evidence of the dependency on stiffness in sensory weighting for proprioceptive sub-modalities, whether applied to a distal (digits) or proximal (shoulder) joint.

The goal of this research is to offer additional evidence regarding the impact of stiffness on sensory integration for both proximal and distal joints. Within environments with increased stiffness, humans tend to prioritize force feedback over position feedback. Further, to examine the role of joint location in this process. We hypothesize that both environment stiffness and joint location significantly affect the sensory weighting process. The first objective of this study is to elaborate on the existing findings that the increase in environment stiffness lead to an increase in the force weighting factors. The second objective is to examine whether proximal joints will yield more accurate force feedback, resulting in relatively higher force weighting factors. Conversely, distal joints provide more accurate position feedback. Or that the opposite is true, where proximal joints will yield more accurate position feedback, resulting in relatively higher position weighting factors, and distal joints will yield more accurate force feedback.

We conducted an analysis of reaching movements using upper body joints in human subjects. These movements were performed specifically with the wrist (vertical palmar flexion), elbow (vertical flexion), and shoulder (vertical retroflexion), with the shoulder representing the most proximal joint and the wrist the most distal. We conducted these experiments in three different stiffness environments while maintaining a consistent testing setup, adjusting only the equipment to accommodate the different joints. This methodology allowed for a precise comparison of how position and force feedback integration varies across these three distinct joints.

Methods and Materials

Participants

Ten healthy female participants, ranging in age from 21 to 24, including one left-handed individual, participated in this study. They were tasked to perform 30 vertical flexion/extension movements for each isolated joint (wrist, elbow, shoulder) in their dominant arm under three distinct stiffness conditions. Before their participation, informed consent was obtained from each participant. The experiment was approved by the Human Research Ethics Committee of the Delft University of Technology.

Experimental Setup

The participants were positioned in a standing position behind a haptic manipulator (HapticMaster, Moog inc. (Van der Linde et al., 2002)). The participant's core was situated beyond the range of motion of the HapticMaster during the experiments to ensure the safety of the participants. The participants held the handle mounted to the HapticMaster, see Appendix A, with their dominant hand, to operate the HapticMaster. In case of wrist movements, the lower arm was fixed. In case of elbow movements, the upper arm was fixed. A wrist brace (Push wrist brace Med 3) was worn to further eliminate the wrist movements in case of the reaches performed with the elbow. This brace consist of a metal frame to eliminate palmar flexion movements of the wrist. For the reaches performed with the shoulder, an additional custom-made brace was worn, Appendix B, along with the wrist brace, effectively isolating vertical retroflexion of the shoulder. Visual feedback displaying the applied forces was presented at eye level, positioned 1.5 meters in front of the participant on a 40-inch monitor with a resolution of 1920 x 1080 pixels. An opaque screen was positioned between the participant's line of sight and the HapticMaster, to obstruct direct visual feedback of movements. Both the height of the screen and the positioning of the upper and/or lower arm attachment points were adjustable to ensure usability for all participants, see Figures 1a – 1c. All participants' arm segment lengths were measured prior to the experiment to verify their compatibility with operating the HapticMaster, as the configuration of the HapticMaster's environment remained unaltered due to time constraints imposed by the overall experiment, see Appendix C. The participants held a trigger button with their non-dominant hand, triggering the initiation of data recording. An emergency button, which switches off the HapticMaster, was positioned at ground level to enable participants to operate it using their feet.

Experimental Approach

Within the haptic virtual environment of the HapticMaster, changing force conditions and consistent predefined

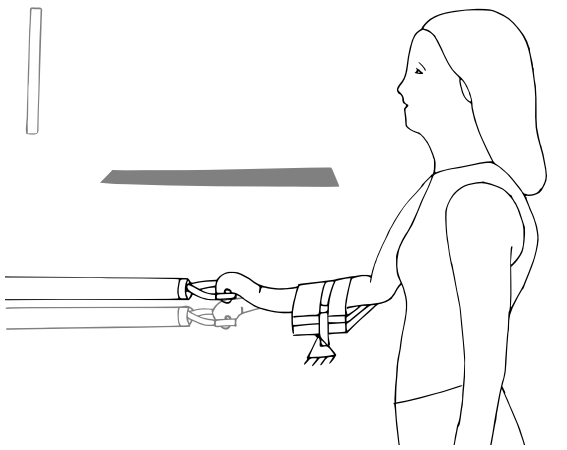

a Experimental setup for reaches with the wrist

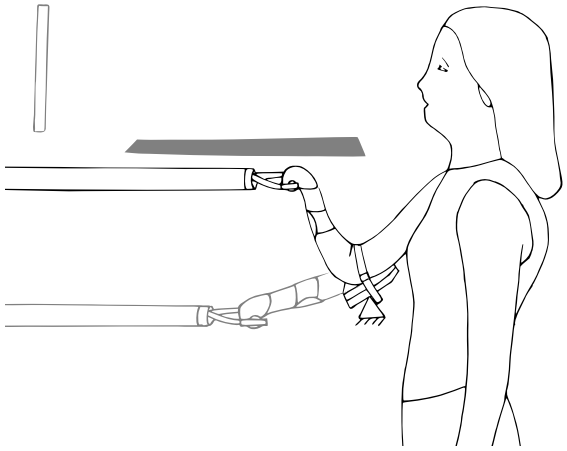

b Experimental setup for reaches with the elbow

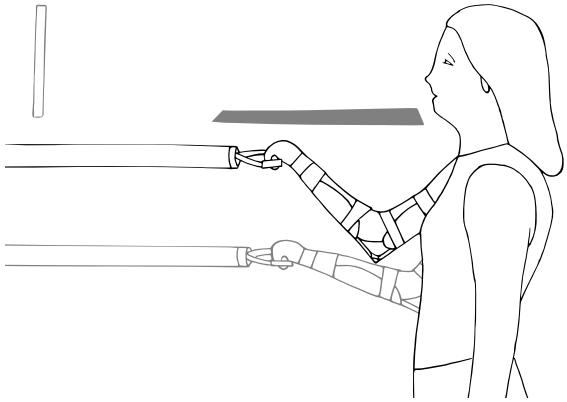

c Experimental setup for reaches with the shoulder

Figure 1. Experimental setup for the three joints studied, where participants were located in a standing position behind the HapticMaster to perform reaching movements. The triangle in the figure indicates a fixed support. For the wrist reaches, the lower arm was fixed. For the Elbow, the upper arm was fixed, and wrist movements were eliminated by the use of a brace. For the shoulder, movements of both the elbow and the wrist were eliminated by the use of two braces. The gray arm sketch represents the arm's position following the reach. As the arm follows the predefined pathways of the HapticMaster, it generates circular movements of the end effector with the center point of that circle being the joint studied.

pathways to follow are created, allowing isolated vertical reaching movements for the wrist (palmar flexion), as well as for the elbow (flexion) and for the shoulder (retroflexion). Virtual objects with exceptionally high stiffness enclose the end effector, giving the operator the sensation of operating within a circular tunnel. When performing the reach, a virtual spring along with a bias force allow for an increasing force at the end effector of the HapticMaster, so that the operator feels as if he/she is pulling a spring. Both the location of the bias force and the virtual attachment position of the spring that are applied to the end effector of the HapticMaster rely on the position of the end effector in two dimensions. These coordinates are employed to compute the angle, denoted as θ, representing the deviation of the end effector from its initial position. The trajectory resembles a circular path, with distinct central points for each joint's rotation to match the rotation point of each joint. θ_{wrist}, θ_{elbow} and $\theta_{shoulder}$ are calculated based on the coordinates from the HapticMaster (x,z) using trigonometric functions, see Appendix D.

The force experienced by the operator, which linearly increases during the rotational movement, is denoted as Equation 1. The stiffness conditions are implemented in N/rad, so that the force is given in N. It is important to note that these are inherently proportional to the moment arm of the circular movement, which varies consistently across the three joints ($d_{wrist} = 0.0615$ m, $d_{elbow} = 0.209$ m, $d_{shoulder} = 0.397$ m). During the experiments, the force at the end effector covertly differs between the linear condition, F_{lin}, and a second condition, where the force increases nonlinearly, F_{nonlin}, as represented in Equation 2.

$$F_{lin} = k_{lin} \cdot \theta \tag{1}$$

$$F_{nonlin} = k_{nonlin}(\theta) \cdot \theta \tag{2}$$

The nonlinear stiffness factor ($k_{nonlin}(\theta)$) is designed so that in the case of small rotational movements, the force difference between the linear and nonlinear spring is small compared to cases where the rotational movement is larger. k_{nonlin}, Equation 3, depends on δ, which in turn is depending on the rotation. δ refers to a constant force difference (F_{nonlin} - F_{lin}) at the position where the linear spring would have exerted the target force. The rotation refers to the angle that the end effector has travelled, and thus refers to the amount of flexion of the joint of the operator, see Equation 4. By design, the nonlinear spring generates a 10% higher force ($\delta = 0.1$) at the target location with respect to

the linear spring. When the target is reached, θ is equal to the rotation needed to reach the target, see Equation 5. Here, $\theta = Rotation$.

$$k_{nonlin} = k_{lin} + \frac{\delta \cdot k_{lin}^2}{Rotation \cdot k_{lin}} \cdot \theta \tag{3}$$

$$\delta = \frac{\theta}{Rotation} \cdot 0.1 \tag{4}$$

$$\begin{aligned} k_{nonlin} &= k_{lin} + \frac{\delta \cdot k_{lin}^2}{Rotation \cdot k_{lin}} \cdot \theta \\ &= k_{lin} + \frac{\frac{\theta}{Rotation} \cdot 0.1 \cdot k_{lin}^2}{Rotation \cdot k_{lin}} \cdot \theta \\ &= k_{lin} + (\frac{\theta^2}{Rotation^2} \cdot 0.1 \cdot k_{lin}) \\ \\ &if \quad \theta = Rotation \\ &= k_{lin} + (0.1 \cdot k_{lin}) \\ &= 1.1 \cdot k_{lin} \end{aligned} \tag{5}$$

When participants unknowingly operate the nonlinear spring and primarily reproduce the position as in the linear situation, they will end up applying a larger force, and they prioritize position feedback. When participants unknowingly operate the nonlinear spring and primarily reproduce the force as in the linear case, they will end up with a smaller rotational movement. If during the experiments, the participants are trying to reach the target, they will integrate position and force feedback, and end somewhere in between these two extremes, see Figure 2. Repeating this for all three joints separately in three distinct stiffness conditions, reveals the weighting strategy and how this is influenced by changing environment stiffness and joint proximity. To analyze the results, the position weighting factors are determined, which are the weights used for the single cue estimate regarding the position feedback in the integration process. They are determined by dividing the force difference between the catch trial (blindly operating the nonlinear spring) and blind trial (blindly operating the linear spring) over the maximal force difference, see Equation 6 and Figure 2. Subsequently, the weighting factor for the force is determined, see Equation 7. With an increasing accuracy of position feedback, the value of W_x increases, and therefore W_f decreases, as both factors sum up to 1. In case that position feedback is prioritized, the information is thought to be more accurate compared to the force feedback and therefore $W_x > 0.5$. Similarly, if force feedback is thought to be more accurate, compared to position feedback, force feedback has a higher influence in the integration process. Now, $W_x < 0.5$ and subsequently, $W_f > 0.5$.

$$W_x = \frac{\Delta y_{catch-blind}}{\Delta y_{max}} \tag{6}$$

$$W_f = 1 - W_x \tag{7}$$

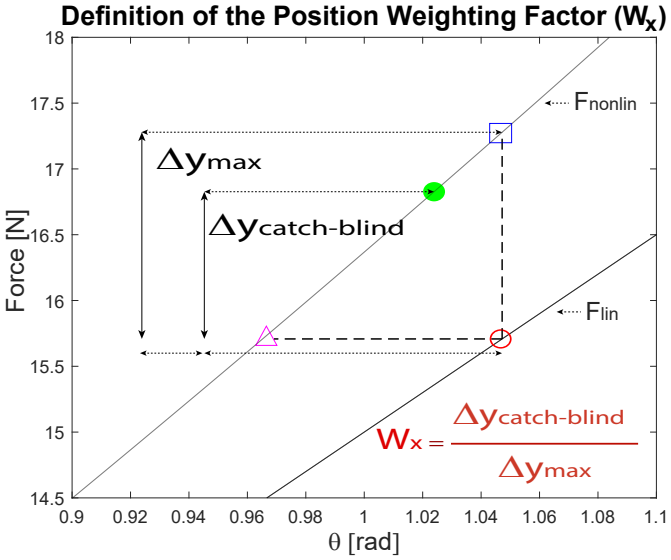

Figure 2. The linear (F_{lin}) and nonlinear (F_{nonlin}) force trajectories plotted against the rotation of the end effector over its predefined path (θ). The red open circle represents the target location. The blue square represents the location where the end effector would end up if the position is fully reproduced, therefore resulting in a higher force than the target force, indicating that position feedback is prioritized. The magenta triangle represents the location where the end effector would end up if the force is fully reproduced, therefore resulting in a smaller rotation compared to the rotation needed to reach the target, indicating that force feedback is prioritized. The green dot represents the location where the end effector actually ends up, and typically lies in between the blue square and the magenta triangle. The force difference between the blue square and the red open circle is indicated by Δy_{max}, and the force difference between the green dot and the red open circle by $\Delta y_{catch-blind}$.

Maximum Likelihood Estimation

The results of the reaching movement experiments are compared to the prediction of the MLE model. Within this model, the position weighting factors and the force weighting factors for all stiffness levels are predicted based on the standard deviation of the feedback cue of that sub-modality (Mugge et al., 2009). Based on the predictions of the MLE model, the weighting factors for position and force are both estimated to be 0.5 at a specific crossover stiffness. To

calibrate the weighting strategy, the experimental stiffness conditions ought to closely approximate this crossover stiffness. The crossover stiffness values for the wrist, elbow and shoulder, are experimentally determined after which three experimental stiffness conditions are selected. These include one at the mean of the crossover stiffness values, another above, and one below.

Experimental Determination of Stiffness Conditions

Participants Two healthy right-handed participants, both 23 years old, one male, one female, participated in this experiment. They were tasked with performing vertical flexion movements to reproduce a target force (referred to as force task) and to reproduce a target position (referred to as position task). Both tasks are performed with the wrist (palmar flexion), elbow (flexion) and shoulder (retroflexion) of the dominant arm of the participant. Prior to their involvement, informed consent was obtained from each participant. The experiment was approved by the Human Research Ethics Committee of the Delft University of Technology.

Experimental Setup For the force task, participants were located behind the same setup as the reaching movements setup (including the braces, opaque screen, feedback monitor, trigger button and emergency button). However, where the participants held the handle of the HapticMaster to perform the reaches, here the participants held an identical handle mounted on the AtiDaq 45 mini force sensor. This sensor is experimentally validated before use, Appendix E. The sensor was oriented such that it measured the force in the vertical direction for each joint. The height of the sensor was adjustable to ensure usability for all three joints as well as for both participants. The visual feedback available on the monitor represented the force exerted on the handle. For the position task, participants were positioned behind the exact same setup as the reaching movements setup. The environment of the HapticMaster included the virtual objects inducing the feeling of operating in a circular tunnel. However, while participants felt like pulling a spring during the reaches, here the spring and bias force were deleted from the environment. The visual feedback available on the monitor represented the amount of rotation the end effector of the HapticMaster had travelled from the starting position.

Experimental Conditions For the force task the participants were asked to reproduce a target force of 15.7 N. They repeated this for six runs, each containing eight trials, alternating four reference trials, where visual feedback was available, and four blind trials, where no visual feedback was available. For the position task, the participants were asked to reproduce a rotation of 2.1 rad from the starting position. They repeated this for six runs, each containing eight trials, alternating four reference trials, where visual feedback was available, and four blind trials, where no visual feedback was available. Both the force and position task were performed with the wrist, elbow and shoulder. Two training runs were included before the start of both tasks. Following MLE, one can estimate the stiffness factors (k), in N/rad, by dividing the standard deviation of the force task results of the blind trials ($\sigma_{(F_{blind})}$) by the standard deviation of the position task results of the blind trials ($\sigma_{(\theta_{blind})}$), see Equation 8 (Körding & Wolpert, 2006; Mugge et al., 2009; Geelen et al., 2023).

$$k = \frac{\sigma_{(F_{blind})}}{\sigma_{(\theta_{blind})}} \tag{8}$$

Experimental Conditions Reaching Movements

The ten participants were asked to reproduce a target force of 15.7 N. After a training session of two runs, both containing eight targets, per stiffness for every joint, the experiment started. A single run contained reference trials, where visual feedback was available representing the exerted force, blind trials, where no visual feedback was available during the reach, and catch trials, where the reach was performed within the nonlinear environment and no visual feedback was available during the reach. When the participants were convinced they applied the same force to the end effector as in the training and reference trials, they pushed the trigger button, after which they returned to the start position (extension of the joint). Participants were instructed to maintain a constant force level during the button press. After each run, which contained four reference trials, two blind and two catch trials, the participants rested for one minute. Each run commenced with a reference trial, randomly followed by either a blind or catch trial. Another reference trial followed this sequence. After ten runs, the stiffness of the environment increased, with a total of three stiffness conditions. The target force remained equal, which means that the rotation needed to reach the target decreased, see Equation 1. Based on the results of the stiffness condition experiment, the stiffness factors are set to 15 N/rad, 50 N/rad and 80 N/rad. Consequently, these stiffness values establish the experimental conditions for the reaching movement experiments, as outlined in Table 1.

Table 1. Consistent target force and variable target rotation (θ) for the three experimental stiffness conditions.

k_{lin} [N/rad]	Target Force [N]	θ [rad]
15	$5 \cdot \pi$	$\pi/3$
50	$5 \cdot \pi$	$\pi/10$
80	$5 \cdot \pi$	$\pi/16$

Maximal Force

As an additional component of the reaching movement experiment, we assessed the maximum voluntary force of each joint for every participant upon the conclusion of all other runs. This assessment allows us to make comparisons among participants regarding the results of weighting factors and maximum capabilities. This evaluation carried out utilizing the AtiDaq 45 mini force sensor. The participants were instructed to exert their maximum force by pushing against the handle connected to the sensor as if they were flexing the joint. The sensor was positioned to measure the force at the target location in the 15 N/rad condition (at $\frac{\pi}{3}$ rad). Additionally, the sensor was aligned to measure the force along the reach direction, parallel to the circular movement path. The arm's bracing, body's positioning, and available feedback mirrored the previous experiment, allowing palmar flexion for the wrist, flexion for the elbow and retroflexion for the shoulder. Consequently, the primary discernible difference for participants, compared to the reaching movement trials, was that they were now required to exert maximal static force, as the handle was in a fixed position. Upon feeling confident about exerting maximum force, participants pressed the trigger button. This was replicated six times for each joint.

Data Analysis

The force levels during the reaching movements are measured for each target, with an average computed over ten data points, comprising five before and five after pressing the trigger button. For all participants, the data is averaged for every specific trial, stiffness and joint type over all similar runs, after exclusion of the failed trials, see Appendix G, resulting in a total of 180 force level values. A Repeated Measures ANOVA is performed to assess the impact of environment stiffness (15 N/rad, 50 N/rad, 80 N/rad), joint type (wrist, elbow, shoulder), and trial type (blind, catch) on the force levels exerted by participants. This test aims to determine whether there are statistically significant variations in participant' exerted force levels in response to changes in stiffness, joint type, or trial type. A second Repeated Measures ANOVA test aimed to test for effects of the joint type and environment stiffness on the difference in the force between the blind and the catch trial (F_{catch}–F_{blind}), as the position weighting factors are calculated based on these differences. To validate these tests, the normal distribution of the two data sets is assessed using both the Kolmogorov-Smirnov and Shapiro-Wilk tests prior to conducting the experiments. Post hoc pairwise comparisons are performed to gain more insight in the level of impact of the stiffness and joint type on both the force levels and force level differences. Cohen's d is manually calculated to reveal the effect sizes of the factors and reveal the effect of the stiffness and joint changes during the experiments (Sullivan & Feinn, 2012). Lastly, a third Repeated Measures ANOVA is conducted to test the effect of joint type and environment stiffness on the deviation from the target ($F_{blind} - F_{target}$), as this deviation is a measure for task difficulty (Bootsma et al., 2018). As task difficulty increases, task performance decreases and therefore deviation from the target increases. All tests are performed using IBM Statistical Packages for Social Sciences Statistics software (v. 29), with a significance level of 0.05.

Results

Stiffness Conditions

The resulting stiffness for every joint, averaged over all trials, is listed in Table 2. The trend is depicted in Figure 3. Joint stiffness demonstrates a rising pattern as the joint's proximity increases. Specifically, the stiffness is greater for the shoulder (average = 61.66 N/rad) when compared to the elbow (average = 51.24 N/rad) and the wrist (average = 29.27 N/rad). Notably, for both participants, the increase in stiffness between the wrist and elbow surpasses the increase in stiffness between the elbow and shoulder. Additionally, both participants exhibit a similar degree of stiffness increase between the wrist and elbow as well as between the elbow and shoulder.

Table 2. Resulting stiffness values for the three joints of both participants.

Participant	Joint	Stiffness [N/rad]
1	Wrist	27.33
	Elbow	46.90
	Shoulder	57.89
2	Wrist	31.21
	Elbow	55.58
	Shoulder	65.43

Reaching Movements: Data Analysis

The Kolmogorov-Smirnov and Shapiro-Wilk test revealed that the data of the force level differences is normally distributed, ($p = 0.200$, $p = 0.476$ respectively). For the force level data set, 5% of the data is identified as outliers (25% or higher deviation from the target) and therefore excluded. After these exclusions the Kolmogorov-Smirnov and Shapiro-Wilk test revealed that the data set including force levels is normally distributed, ($p = 0.200$, $p = 0.060$ respectively). For the Repeated Measures ANOVA on the force level data set, the excluded outliers are estimated as the mean of the remaining data points.

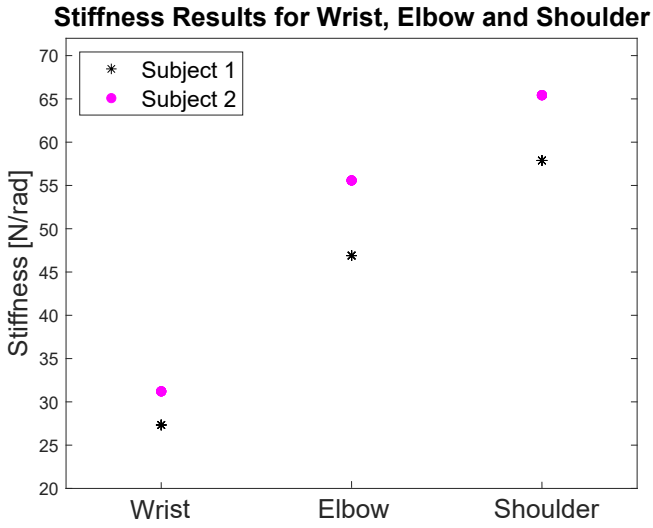

Figure 3. Stiffness values for the three joints studied for both participants, averaged over all trials. An ascending trend is evident as the joint is more proximal (wrist - elbow - shoulder).

Based on the first Repeated Measures ANOVA test, both stiffness as well as trial type show a significant effect on the force levels exerted by the participants as the within subjects' effects reveal a significance of $p = 0.002$ for the stiffness conditions (15 N/rad, 50 N/rad or 80 N/rad) and $p < 0.001$ for the trial type. However, $p = 0.127$ for joint type which indicates no statistically significant effect. In the post hoc comparisons, Cohen's d values reveal that both the increase of 15 N/rad to 50 N/rad and the increase of 50 N/rad to 80 N/rad stiffness conditions show a medium effect on the force levels, Cohen's d = -0.755, Cohen's d = -0.538 respectively, as defined by Sullivan and Feinn (2012). In addition, the change from wrist to elbow has an medium effect on the force levels, Cohen's d = 0.718, and the change from elbow to shoulder has a low effect on the force levels, Cohen's d = -0.367.

The second Repeated Measures ANOVA test revealed that within subjects, stiffness as well as joint type have a statistically significant impact on the force differences between the blind and catch trials, and thus on the weighting factors of position and force feedback, as $p < 0.001$ for the stiffness and $p = 0.020$ for the joint type. When transitioning from 15 N/rad to 50 N/rad, Cohen's d is equal to 1.511, whereas the shift from 50 N/rad to 80 N/rad yields a Cohen's d of 0.355. This indicates a high effect on sensory weighting when stiffness increases from 15 N/rad to 50 N/rad and a small effect when it increases from 50 N/rad to 80 N/rad. Significantly, the positive mean differences of the force differences (catch - blind) observed between 15 N/rad and 50 N/rad, 0.535, as well as between 50 N/rad and 80 N/rad, 0.148, reveal that the force disparity between catch and blind trials diminishes with increasing stiffness conditions. When the force difference decreases, the positional weighting factor decreases, as shown in Figure 2. The effect size of wrist to elbow is high, Cohen's d = -0.867, however the effect size of elbow to shoulder is low, Cohen's d = 0.090. Pairwise comparisons of the three joints reveal that the wrist shows the lowest force difference compared to the elbow and shoulder, as the mean difference between the wrist and elbow is -0.373, and between the wrist and shoulder is -0.340.

Reaching Movements: Data Comparison

The position weighting factors are determined based on the mean results from all participants, as outlined in Figure 2. The results for all three joints under the three stiffness conditions can be found in Figure 4, and the corresponding weighting factors in Table 3. The averaged results for the position weighting factor, W_x, for all three joints in the three stiffness conditions including error bars, representing one standard deviation across all participants, are visualized in Figure 6. In case of the 15 N/rad stiffness condition, the maximum difference between the average position weighting factor is $\Delta W_{x_{max_{elbow-shoulder}}} = 0.06$. The 50 N/rad condition has a maximum difference between the average position weighting factor of $\Delta W_{x_{max_{wrist-shoulder}}} = 0.35$. For the 80 N/rad condition, the maximum difference between the average position weighting factor is $\Delta W_{x_{max_{wrist-elbow}}} = 0.36$.

Table 3. Resulting position and force weighting factors (W_x and W_f respectively) for the three joints studied, averaged over all participants (N=10).

Joint	Stiffness [N/rad]	W_x	W_f	SD
Wrist	15	0.62	0.38	0.29
	50	0.05	0.96	0.35
	80	-0.04	1.04	0.32
Elbow	15	0.68	0.32	0.39
	50	0.33	0.67	0.30
	80	0.32	0.68	0.29
Shoulder	15	0.62	0.38	0.11
	50	0.39	0.61	0.16
	80	0.21	0.79	0.24

Operating in a stiffer environment, results in a higher target overshoot, see Figure 4. In the blind trials, the force, as well as the position is underestimated, resulting in an overshoot of the target. This overshoot is indicated as $\Delta F_{blind-target}$ and increases as the stiffness factor increases. An overshoot of the target is noted in all cases, except for the elbow in the 15 N/rad condition, where the force and

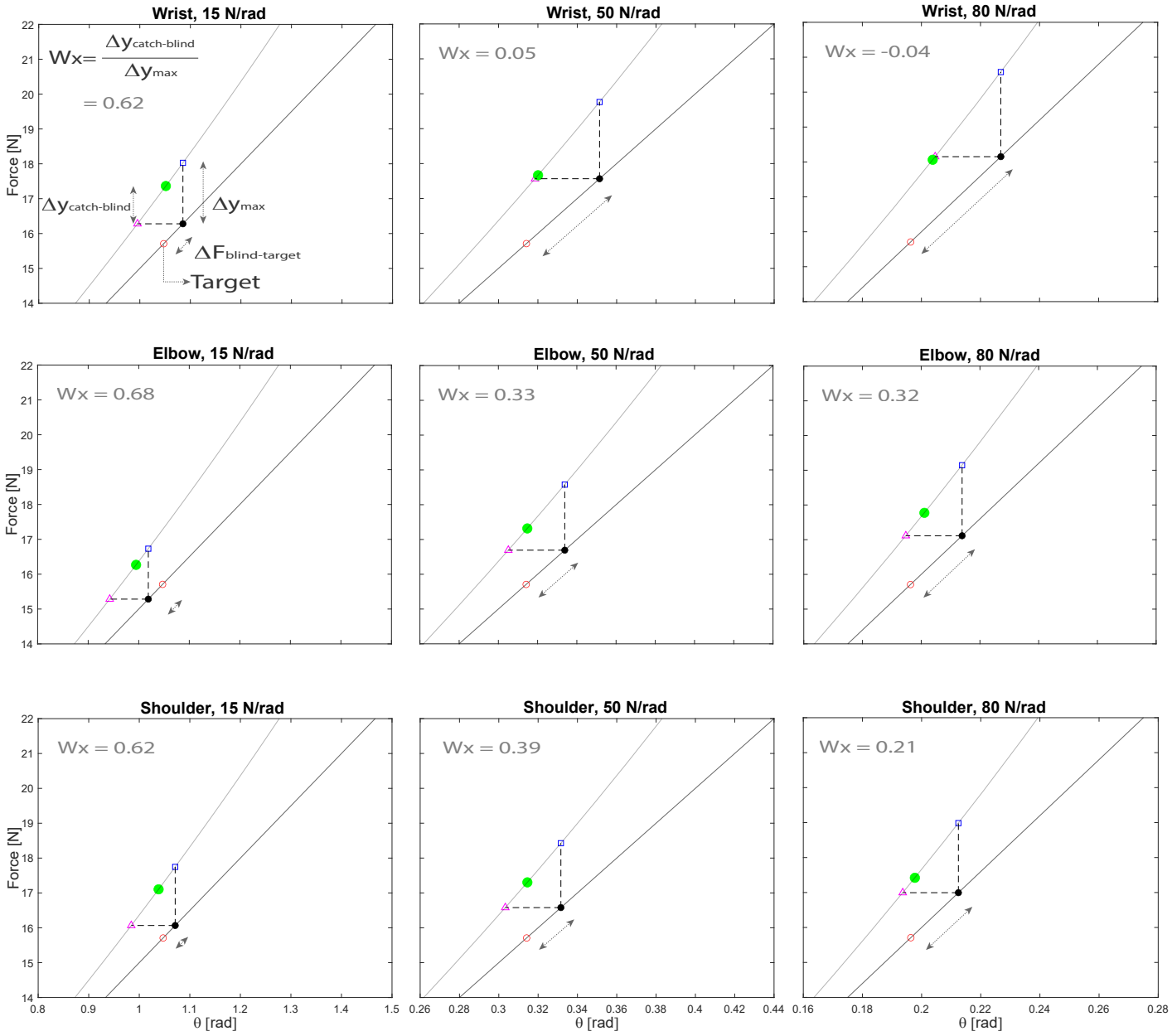

Figure 4. The averaged outcomes across all participants and trial iterations for the wrist, elbow, and shoulder within all three stiffness environments. Three types of trials are included, (1.) reference trial, where the participants control the linear spring and visual feedback is available, (2.) blind trial, where no visual feedback is available, (3.) catch trial, where participants unknowingly control the nonlinear spring without access to visual feedback. The open red circle is the target location, at 15.7 N. The target angle (θ) differs in the three stiffness conditions due to the consistent target force ($\frac{\pi}{3}$, $\frac{\pi}{10}$, $\frac{\pi}{16}$ for 15 N/rad, 50 N/rad, 80 N/rad, respectively). The black dot represents the location where participants ended up in the blind trials. The blue square is the location where participants would end up in the catch trials if the position is exactly reproduced. The pink triangle is the location where participants would end up in the catch trials if the force is exactly reproduced. The green dot is the location where the participants actually ended up in the catch trials. The position weighting factor, W_x, is established based on the green dot's placement, and an analysis of the weighting strategy ensues.

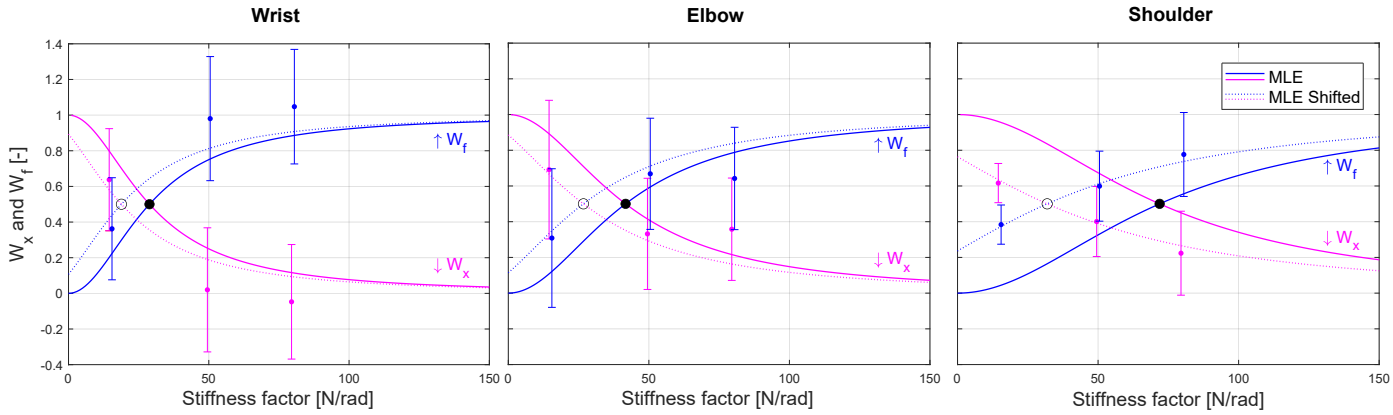

Figure 5. One standard deviation across all participants of the position and force weighting factors for all three stiffness conditions is represented in the error bars. The MLE model predictions for the position and force weighting factor are plotted across the results. The dotted lines represent the shifted model predictions to match the results. The black dot indicates the crossover stiffness of the MLE model prediction. The open black circle indicates the crossover stiffness of the shifted MLE model prediction.

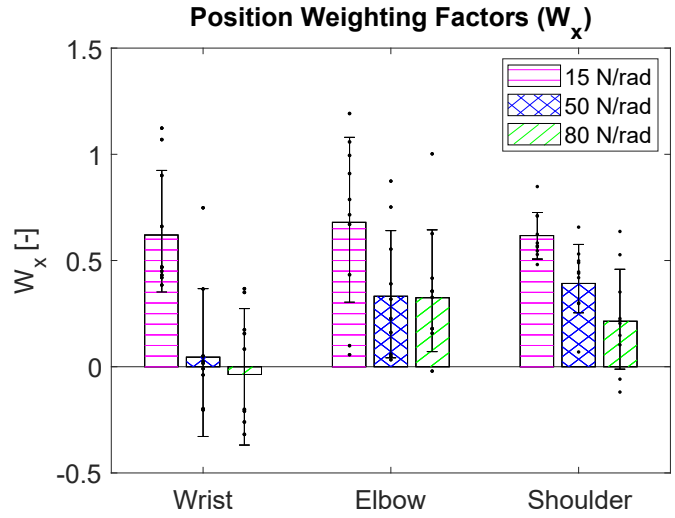

Figure 6. The averaged (N= 10) position weighting factors (W_x) for each joint studied in the three stiffness conditions. The error bars represent one standard deviation of the results of all participants. The black dots represents the position weighting factor for each individual participant.

position are overestimated, resulting in an undershoot of the target. Both stiffness as well as joint type reveal a statistically significant effect on the deviation from the target ($p = 0.011$, $p < 0.001$ respectively). The negative mean difference of the target overshoot (blind trial force - target force) between 15 N/rad and 50 N/rad, as well as between 50 N/rad and 80 N/rad, -1.069 and -0.474 respectively, indicate that an increase in stiffness condition reveals an increase in target overshoot. The positive mean difference of the target overshoot between wrist and elbow as well as between wrist and shoulder, 0.969 and 0.785 respectively, indicates that the wrist represents the highest target overshoot. The negative mean difference of the target overshoot between the elbow and shoulder, -0.184, indicates that the elbow has a lower target overshoot compared to the shoulder.

Maximum Likelihood Estimation

The MLE, based on the average values of the standard deviation of the two participants of the stiffness conditions experiment, is plotted over the results of both averaged W_x and W_f values, see Figure 5. The dotted lines represent the shifted MLE prediction to match the results. For all three joints, the crossover stiffness exhibits an ascending trend as the joint is located more proximal, see Table 4. Appendix F contains the two distinct Maximum Likelihood Estimations for both participants.

Table 4. Crossover stiffness values of both MLE prediction and the shifted MLE model

Joint	MLE crossover stiffness [N/rad]	shifted MLE crossover stiffness [N/rad]
Wrist	28.86	18.86
Elbow	41.72	26.73
Shoulder	71.90	31.90

Maximal Force

The results for the static voluntary maximal force values for palmar flexion of the wrist, flexion of the elbow and retroflexion of the shoulder, averaged over all trials of each participant, can be found in Figure 7. The error bars indicate one standard deviation of the averaged values of all participants. The maximal force exerted by the joints decreases as the joint is located more proximal, as $F_{max_{wrist}} = 63.94\ N$, $F_{max_{elbow}} = 50.46\ N$, and $F_{max_{shoulder}} = 48.32\ N$.

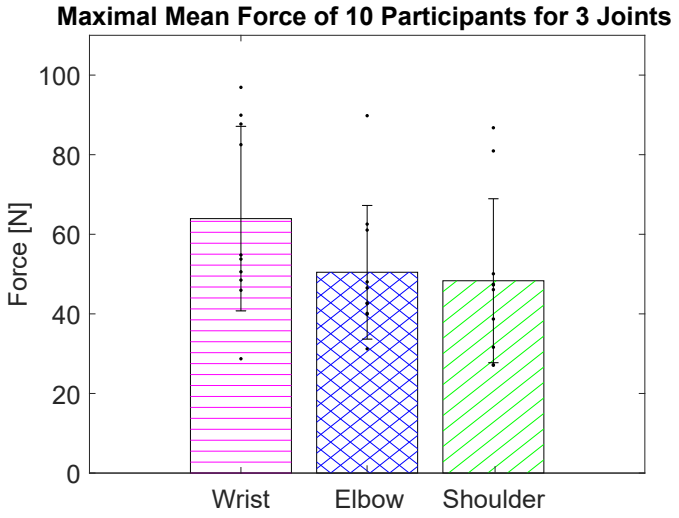

Figure 7. The bars represent the mean experimental maximal force for each examined joint, averaged over all trials. Black dots signify the maximum force achieved by individual participants, and the error bars represent one standard deviation.

Normalized Results

The three experimental stiffness conditions (15 N/rad, 50 N/rad and 80 N/rad) are normalized by dividing over 1.) the experimentally found joint stiffness, averaged across the two participants, see Table 2, and 2.) the experimentally found maximal force, averaged over the ten participants, see Figure 7, times the moment arm of the distinct joint, ($d_{wrist} = 0.0615$ m, $d_{elbow} = 0.209$ m, $d_{shoulder} = 0.397$ m). The results can be found in Table 5.

Table 5. Experimental environment stiffness conditions normalized over the averaged joint stiffness (N=2) and over the averaged maximal force (N=10) times the moment arm of the distinct joint.

Joint	Exp. Stiffness Normalized over Joint Stiffness	Exp. Stiffness Normalized over (Maximal Force · Moment Arm)
Wrist	0.51	3.82
	1.71	12.72
	2.73	20.34
Elbow	0.29	1.42
	0.98	4.74
	1.56	7.59
Shoulder	0.24	0.78
	0.81	2.60
	1.30	4.16

Discussion

The findings provide support for the previously demonstrated trends regarding the influence of stiffness on sensory weighting strategies in human motor control. Consistently across all three joints, the position weighting factor, denoted as W_x, exhibits a discernible decrease as the stiffness factor increases. This implies that as the environment becomes stiffer, participants rely less on positional information and place greater emphasis on force feedback. Subsequently, the force weighting factor, denoted as W_f, displays an upward trend alongside escalating stiffness conditions, indicating a heightened reliance on force when operating within higher stiffness environments. More evidence for this is found in the positive mean differences of the force differences (catch - blind) in the pairwise comparisons. The higher the stiffness of the environment, the more decrease in force level differences between the catch and the blind trial. The weighting of force and position shifts towards force feedback, as this difference decreases. The positive mean difference between the 15 N/rad and 50 N/rad condition is higher compared to the positive mean difference between the 50 N/rad and 80 N/rad condition, logically due to the higher increase in stiffness between 15 N/rad and 50 N/rad compared to the increase in stiffness between 50 N/rad and 80 N/rad.

It is worth noting that the wrist can generate the greatest static force in comparison to the elbow and shoulder. This peak force decreases as the joint is more proximal. The decrease in force can be explained by the wrist having a shorter moment arm in contrast to the longer moment arms of the elbow and shoulder. Consequently, the torque applied is lowest at the wrist and highest at the shoulder. In addition, the participants are required to exert maximum static voluntary force. In case of the shoulder, this force is transferred to the wrist since the wrist is integral in carrying out movements initiated at the shoulder. Therefore, the wrist must always be capable of withstanding the static forces transmitted from the shoulder.

For all three joints, the position weighting factor demonstrates values both above and below the 0.5 threshold, providing clear indications of appropriately selected stiffness conditions, as depicted in Figure 5. It is important to highlight, that across all three joints, the experimentally crossover stiffness consistently falls short when compared to the values predicted by the MLE model. The position weighting factors are lower, and the force weighting factors higher. The effect of heightened force weighting factors compared to the MLE model prediction is stronger for the shoulder, compared to the elbow and is even lower for the

wrist. Thus, where position feedback is weighted lower, more weight is put on force feedback, indicating a higher reliance on force feedback, and this effect seems to increase as the joint is more proximal.

Interestingly, for the wrist, in stiffness conditions 50 N/rad and 80 N/rad, the position weighting factor decreases to a value around zero, which indicates that position feedback does not, or very little, influences the overall proprioceptive estimate. Subsequently, force feedback would for the most part provide the integrated estimate in these conditions. Both 50 N/rad and 80 N/rad are far above the crossover stiffness for the wrist, as predicted by the MLE model. Therefore, the emphasis on force feedback in higher stiffness conditions can be explained for the wrist. For the elbow and shoulder, the position feedback does decrease in the 50 N/rad and 80 N/rad environment but not towards zero, as these stiffness conditions are closer to the crossover stiffness of both joints. However, for the elbow, the position weighting factor does not decrease as much in the middle and high stiffness environment, but flattens, emphasizing force feedback more than predicted by the MLE model. Nonetheless, because the stiffness conditions vary by different amounts from the crossover stiffness for the three joints, the stiffness conditions are relative higher for the wrist compared to the elbow and shoulder. Consequently, a direct comparison between the weighting factors is not feasible, but they should be considered relative to the MLE model predictions. Additionally, the post hoc comparisons of joint type on force level differences (catch-blind) do not directly reveal the influence of joint location on the weighting strategy, but need to be interpreted relative to the model predictions.

For the 15 N/rad stiffness conditions, all three averaged weighting factors are around the same value, $W_{x_{wrist}} = 0.62$, $W_{x_{elbow}} = 0.68$, $W_{x_{shoulder}} = 0.62$, see Table 3. However, 15 N/rad is relatively closer to the crossover stiffness for the wrist compared to the elbow and is even further for the shoulder. Within this stiffness condition, the emphasis on position feedback is relatively higher in the wrist compared to the elbow and shoulder. Following MLE predictions, the shoulder should emphasize the position feedback more as 15 N/rad is relatively lower for the shoulder than for the wrist, and therefore the position weighting factors should be closer to 1. One would expect an increasing W_x in a stiffness condition located further from the crossover stiffness, which is not the case when comparing the wrist, elbow and shoulder in the 15 N/rad condition. This shows preliminary findings that the more distal the joint is, the more accurate position feedback is. The wrist should indicate lower position feedback emphasis, however, W_x values reveal that the position feedback is still highly accurate in this condition.

A similar argument holds when comparing wrist, elbow and shoulder in the 80 N/rad stiffness condition. In the 80 N/rad condition, the force weighting factor is expected to be higher for the elbow, as the stiffness condition is further away from its crossover stiffness (higher) for the elbow compared to the shoulder. However, from Table 3, we observe that the average force weighting factor for the elbow is lower in the 80 N/rad stiffness condition compared to the shoulder in the 80 N/rad stiffness condition, indicating a heightened reliance on position feedback for the elbow. The elbow shows a lower force weighting factor compared to the MLE model prediction for the 80 N/rad condition, indicating a heightened reliance on position feedback. These heightened position weighting factors compared to the MLE model predictions are not discernible for the shoulder in the 80 N/rad stiffness condition.

To give an accurate comparison of the results for the wrist, elbow and shoulder, not only should they be compared to the MLE model predictions, but the differences in maximal voluntary force and joint stiffness of each specific joint must be taken into account. Upon examination of the normalized experimental stiffness conditions, factoring in both joint stiffness and the maximum force multiplied by the moment arm, it becomes evident that the experimental stiffness conditions exhibit relative differences across the three joints, as shown in Table 5. As a result, directly comparing the weighting factors of the wrist at 15 N/rad with those of the elbow at 15 N/rad and shoulder at 15 N/rad is not feasible. A more appropriate strategy would involve comparing the results for the wrist at 15 N/rad to the results for the elbow and shoulder at 50 N/rad and 80 N/rad, respectively, as the normalized experimental conditions over the maximal force times the moment arm are more alike (3.82, 4.74, 4.16 for the wrist, elbow, and shoulder, respectively). Similarly, when assessing the results for the wrist at 50 N/rad, it would be more appropriate to compare them with the results for the elbow and shoulder at 80 N/rad, as the normalized experimental conditions over the joint stiffness are more alike (1.71, 1.56, 1.30 for the wrist, elbow, and shoulder, respectively). Comparing the wrist at 15 N/rad with the elbow at 50 N/rad and the shoulder at 80 N/rad, the position weighting factors that follow are, $w_{x_{wrist}} = 0.62$, $w_{x_{elbow}} = 0.33$, $w_{x_{shoulder}} = 0.21$. Thus, when accounting for the differing maximal force as well as moment arm, the more proximal the joint (wrist to shoulder), the lower the position weighting factor becomes. Comparing the wrist at 50 N/rad to the elbow and shoulder at 80 N/rad, the

position weighting factors that follow are, $w_{x_{wrist}} = 0.05$, $w_{x_{elbow}} = 0.32$, $w_{x_{shoulder}} = 0.21$. The decreasing position weighting factors with increasing joint proximity when accounting for the joint stiffness is only valid when comparing the elbow and shoulder. One plausible explanation for this observation is that the task is exceptionally challenging for the wrist in the 50 N/rad and 80 N/rad stiffness condition. As sensory integration is an asymmetric process, the nervous system selectively prioritizes force feedback over position feedback based on its relative importance to achieve the task of reproducing the target force (Logan et al., 2014).

Additionally to the observations that the wrist reveals an increase in force weighting factors with increasing stiffness conditions, the overshoot of the target increases significantly the more distal the joint is located, as well as with increasing stiffness conditions. Increasing target overshoot suggests that the task carried out with the wrist and in higher stiffness conditions indeed poses the greatest challenge, as performance decreases. An increase in task difficulty for the wrist is supported by the observation that the standard deviation across participants is higher for the wrist compared to the shoulder.

An explanation for the decrease in position weighting factors as joint proximity increases can be found in the biomechanics differences between proximal and distal joints. As proximal joints have a higher density of proprioceptors, arguably the Just Noticeable Difference is smaller for proximal joints compared to distal joints. The Just Noticeable Difference (JND), is a measure of the smallest change in sensory input that can be reliable detected by the observer (Kroemer Elbert et al., 2018). More proximal joints can therefore detect smaller changes in joint deflection. The higher sensitivity of sensory information from proximal joints is important for the control of limb movement, as it allows the CNS to quickly respond to small changes in limb position and movement direction. In contrast, the lower sensitivity of sensory information from distal joints allows for greater flexibility of limb movement. As the JND is lower for proximal joints, the position of the joint is less altered to detect changes compared to distal joints, which need a larger deflection of the joint to detect changes. Furthermore, the deflection of a joint at the shoulder exerts a significant influence on the positioning of the digits, primarily due to the substantial moment arm associated with this joint. In contrast, a joint deflection at the wrist has a comparatively minor impact on digit positioning. Consequently, there is a strong preference for a higher accuracy in feedback regarding joint deflection at the shoulder, as it plays a critical role in the precise control of arm movements.

Mugge et al. (2009) argued that when an object is stiff, the emphasis shifts to force feedback, as the deflection of the object when grasping the object is minimal. Consequently, the joint deflection is low and the orientation of the joint remains (almost) unaltered. The emphasis towards force feedback increases, and as the JND of proximal joints is lower, proximal joints are considered to reveal more accurate force feedback. Similarly, as the JND in distal joints is higher, a higher deflection of the distal joint is needed before the change in position or force is detected, resulting in a higher positional error, and therefore position feedback is considered to be more accurate. The same argument is made by Drewing and Ernst (2006), who presented sensory weighting of force and position feedback during active touch. When the object is curved, position feedback is given more weight in the integration process compared to when the object is flat. When touching a flat object, force feedback is up-weighted. Considering the minimal joint deflection when touching a flat object, explains for the emphasizing of force feedback when touching a flat object. It is therefore argued that force feedback accuracy increases the more proximal the joint, as the joint deflection is only minimal when the nervous system detects it. For distal joints, the joint deflection is already larger before the nervous system detects it, due to a higher JND, resulting in higher accuracy towards position feedback.

Limitations

Sensory weighting in human motor control is influenced by various factors, such as environmental conditions, task demands, attention, and prior beliefs. A strict approach was needed to reveal the effects of environment stiffness and joint location on the weighting of position and force feedback. Meaning, the experimental setup was only adjusted to accommodate the three distinct joint, while maintaining other factors consistent, such as environment and task instructions. However, limitations emerged during the experiments, which possibly influenced the weighting strategy.

Braces are worn with the intention of restricting wrist movements in the case of the elbow experiment and curtailing both elbow and wrist movements in the case of the shoulder experiment. It is important to note that the wrist brace is specifically designed to restrict palmar and dorsal flexion of the wrist without completely immobilizing the joint. As a result, some degree of movement persists during the experiment, providing a certain level of sensory feedback that could potentially impact the sensory weighting for the elbow and shoulder.

Notably, uniform stiffness conditions have been em-

ployed across all participants, yet disparities persist in terms of joint stiffness and maximum force output among individuals. Consequently, the imposed stiffness conditions and targeted force levels present varying degrees of challenge among participants. In order to minimize these discrepancies, exclusive enrollment of female subjects aged 21 to 25 has been implemented. This focused participant selection aims to curtail variations, thereby promoting greater uniformity within the study. However, the maximal force for every joint, per participant, revealed that the maximal differences between participants is still 68.1969 N for the wrist, 58.5843 N for the elbow and 59.6725 N for the shoulder.

Furthermore, the stiffness conditions (15 N/rad, 50 N/rad, 80 N/rad) are uniformly applied to all joints. As demonstrated, the shoulder exhibits higher experimental stiffness values in comparison to the elbow and wrist. It is evident that the shoulder's crossover stiffness surpasses that of the elbow and wrist. Consequently, the experimental stiffness conditions are relatively lower for the shoulder and higher for the wrist. When assessing the weighting factors, this relationship should be taken into consideration to accurately determine whether force or positional information is given more weight. To enhance the precision of this comparison, a more effective approach may involve adjusting the experimental stiffness conditions for each joint, ensuring they deviate from their crossover stiffness by a consistent amount.

For all participants, the same experimental protocol is used, meaning the shoulder is analyzed lastly for all participants, as well as the 80 N/rad condition. Mental tiredness could have decreased the attention of the participants. As attention is indicated to be a factor that influences the sensory weighting process during human motor control (Block & Bastian, 2010), this could have influenced the results of this research. In addition, muscle tiredness may have influenced the weighting strategy in the 80 N/rad condition. Both attention decrease and muscle tiredness are mitigated as much as possible in the time range of these experiments, by implementing short breaks after each trial, and longer breaks in between the trials with the three joints as well as in between the stiffness conditions.

The three rotations needed to reach the target (in the blind and reference trials), are $\pi/3$ rad in the 15 N/rad condition, $\pi/10$ rad in the 50 N/rad condition, and $\pi/16$ rad in the 80 N/rad stiffness condition. These rotations remain the same for each joint, as both the target force as well as the stiffness conditions remain consistent. However, the shoulder joint has a greater maximal range of motion ($\sim\pi$ rad) compared to the elbow ($\sim 0.72\pi$ rad) and wrist ($\sim 0.5\pi$ rad) (Chang et al., 2023; Zwerus et al., 2019; Gates et al., 2016). Although all experimental range of motions are well below the maximal range of motions, the experimental range of motions are relatively larger for the wrist compared to the elbow and shoulder, as the maximal range of motion is smaller.

Conclusion

We hypothesized that both environment stiffness and joint proximity significantly impacted the sensory weighting of force and position feedback. Further, this study 1.) elaborates on the existing findings that an increase in environment stiffness lead to an increase in the force weighting factors, and 2.) it examines whether force or position feedback is up-weighting in more proximal joints. We accept our hypothesis regarding the influence of environment stiffness and joint location on the sensory weighting process of force and position feedback as stiffness condition and joint location reveal a statistically significant effect on the force level differences (catch - blind), ($p < 0.001$, $p = 0.020$ respectively.)

Regarding our first objective, as stiffness conditions rise, there is a noticeable downward trajectory in the position weighting factors. As stiffness conditions increase, the accuracy of force feedback improves, resulting in heightened force weighting factors. Additional pairwise comparisons reveal that the 15 N/rad shows higher force differences (catch - blind), due to its positive mean difference, compared to the 50 N/rad condition. This indicates higher position weighting factors, indicating a heightened reliance on position feedback in the 15 N/rad condition. The same argument holds for the 50 N/rad compared to the 80 N/rad condition, revealing higher force differences (catch - blind) for the 50 N/rad compared to the 80 N/rad. This study presents further evidence that increasing stiffness conditions lead to decreasing position weighting factors and an increase in reliance on force feedback.

Turning to our second objective, we present encouraging findings concerning the impact of joint proximity on the weighting factors. In the 15 N/rad stiffness condition, the wrist reveals relatively higher position weighting factors when relating to the MLE model predictions, compared to both the elbow and shoulder. Statistical evidence regarding the increase in position weighting factors for more distal joints is non existing as the results should be considered relatively to the MLE model predictions. Comparing the results relatively to the MLE predictions, it is observed that during the integration process, the wrist assigns a greater

weight to the position feedback compared to the elbow and the elbow in turn, assigns a greater weight to the position feedback compared to the shoulder. This phenomenon is exemplified in the low stiffness conditions. The position weighting factor is heightened for the wrist compared to the MLE model predictions. The degree of increase relative to the MLE model prediction is less pronounced for the elbow and even more subdued for the shoulder. Further, observing the normalized experimental stiffness conditions, and subsequently comparing the wrist at 15 N/rad, with the elbow at 50 N/rad and shoulder at 80 N/rad, it is revealed that the more proximal the joint, the lower the position weighting factors. For the comparison of the results of the wrist at 50 N/rad and the elbow and shoulder at 80 N/rad condition, the higher position weighting factor is not observed for the wrist, when compared to the elbow and shoulder, but this is due to the exceptionally high task difficulty for the wrist in high stiffness environments.

The research exhibited how isolated vertical reaching movements, involving palmar flexion of the wrist, flexion of the elbow and retroflexion of the shoulder, reveal stiffness-dependency in the sensory integration process, encompassing both force and position feedback. As environment stiffness increases, the shift from higher position weighting factors to higher force weighting factors is observed. Moreover, this study offered preliminary evidence that joint proximity also impact the sensory integration, up-weighting force feedback when joint proximity increases.

Acknowledgements

I would like to thank all the participants of this study for their time and cooperation. Additionally, I would like to express my appreciation to Dr. ir. W. Mugge for the valuable insights and support he provided to this project. Also, I would like to acknowledge Dr.ir. A.H.A. Stienen, J.E. Geelen and A.A.M. van der Kraan for their help regarding the HapticMaster. Finally, I want to extend my thanks to the NMClab members for their valuable discussions on the subject and for providing access to the necessary equipment for our experiments.

References

Alais, D., & Burr, D. (2019). Cue Combination Within a Bayesian Framework. In *Multisensory processes* (pp. 9–31). Springer, Cham. Retrieved from https://link.springer.com/chapter/10.1007/978-3-030-10461-0_2 doi: 10.1007/978-3-030-10461-0{_}2

Block, H. J., & Bastian, A. J. (2010, 1). Sensory Reweighting in Targeted Reaching: Effects of Conscious Effort, Error History, and Target Salience. *Journal of Neurophysiology*, *103*(1), 206–217. Retrieved from /pmc/articles/PMC2807220//pmc/articles/PMC2807220/?report=abstracthttps://www.ncbi.nlm.nih.gov/pmc/articles/PMC2807220/ doi: 10.1152/JN.90961.2008

Block, H. J., & Bastian, A. J. (2011, 7). Sensory weighting and realignment: independent compensatory processes. *J Neurophysiol*, *106*(1), 59–70. Retrieved from www.jn.org doi: 10.1152/jn.00641.2010.-When

Bootsma, J. M., Hortobágyi, T., Rothwell, J. C., & Caljouw, S. R. (2018, 9). The Role of Task Difficulty in Learning a Visuomotor Skill. *Medicine and science in sports and exercise*, *50*(9), 1842–1849. Retrieved from https://pubmed.ncbi.nlm.nih.gov/29634641/ doi: 10.1249/MSS.0000000000001635

Chang, L.-R., Anand, P., & Varacallo, M. (2023). *Anatomy, Shoulder and Upper Limb, Glenohumeral Joint*. StatPearls Publishing. Retrieved from https://www.ncbi.nlm.nih.gov/books/NBK537018/

Drewing, K., & Ernst, M. O. (2006). Integration of force and position cues for shape perception through active touch. *Brain research*, *1078*(1), 92–100. Retrieved from https://pubmed.ncbi.nlm.nih.gov/16494854/ doi: 10.1016/j.brainres.2005.12.026

Ernst, M. O., & Banks, M. S. (2002, 1). Humans integrate visual and haptic information in a statistically optimal fashion. *Nature*, *415*(6870), 429–433. Retrieved from https://pubmed.ncbi.nlm.nih.gov/11807554/ doi: 10.1038/415429A

Fei Yam, M., Chun Loh, Y., Shan Tan, C., Khadijah Adam, S., Abdul Manan, N., & Basir, R. (2018, 7). General Pathways of Pain Sensation and the Major Neurotransmitters Involved in Pain Regulation. *International Journal of Molecular Sciences*, *19*(8), 2164. Retrieved from www.mdpi.com/journal/ijms doi: 10.3390/ijms19082164

Gates, D. H., Walters, L. S., Cowley, J., Wilken, J. M., & Resnik, L. (2016). Range of Motion Requirements for Upper-Limb Activities of Daily Living. *The American Journal of Occupational Therapy*, *70*(1), 1–7001350010. Retrieved from http://dx.doi.org/ doi: 10.5014/ajot.2016.015487

Geelen, J. E., Van Der Helm, F. C. T., Schouten, A. C., & Mugge, W. (2023). Sensory weighting of position and force feedback during pinching. *Exp Brain Res*, *241*, 2009–2018. Retrieved from https://doi.org/10.1007/s00221-023-06654-1 doi: 10.1007/s00221-023-06654-1

Hatsopoulos, N. G., Olmedo, L., & Takahashi, K. (2010, 12). Proximal-to-Distal Sequencing Behavior and Motor Cortex. In *Motor control: Theories, experiments, and applications*. Oxford University Press. Retrieved from https://academic.oup.com/book/8542/chapter/154407040 doi: 10.1093/ACPROF:OSO/9780195395273.003.0007

Hoffman, M., & Gregory Payne, V. (1995). The Effects of Proprioceptive Ankle Disk Training on Healthy Subjects. *The Journal of orthopaedic and sports physical therapy*, *21*(2), 90–93. Retrieved from www.jospt.org

Hudson, H. M., Park, M. C., Belhaj-Saïf, A., & Cheney,

P. D. (2017, 7). Representation of individual forelimb muscles in primary motor cortex. *J Neurophysiol*, *118*(1), 47–63. Retrieved from www.jn.org doi: 10.1152/jn.01070.2015.-Stimulus-triggered

J Smeets, J. B., van den Dobbelsteen, J. J., J de Grave, D. D., van Beers, R. J., & Brenner, E. (2006). Sensory integration does not lead to sensory calibration. *Proceedings of the National Academy of Sciences of the United States of America*, *103*(49), 18781–18786. Retrieved from www.pnas.orgcgidoi10.1073pnas.0607687103

Körding, K. P., & Wolpert, D. M. (2004, 1). Bayesian integration in sensorimotor learning. *Nature 2004 427:6971*, *427*(6971), 244–247. Retrieved from https://www.nature.com/articles/nature02169 doi: 10.1038/nature02169

Körding, K. P., & Wolpert, D. M. (2006, 7). Bayesian decision theory in sensorimotor control. *Trends in Cognitive Sciences*, *10*(7), 319–326. Retrieved from https://pubmed.ncbi.nlm.nih.gov/16807063/ doi: 10.1016/J.TICS.2006.05.003

Kroemer Elbert, K. E., Kroemer, H. B., & Kroemer Hoffman, A. D. (2018, 1). Human Senses. *Ergonomics*, 171–252. Retrieved from https://www.sciencedirect.com/science/article/pii/B9780128132968000050 doi: 10.1016/B978-0-12-813296-8.00005-0

Landy, M. S., Laurence, ., Maloney, T., Johnston, E. B., & Young, M. (1995). Measurement and Modeling of Depth Cue Combination: in Defense of Weak Fusion. *Vision research*, *35*(3), 389–412. Retrieved from https://www.sciencedirect.com/science/article/pii/004269899400176M?via%3Dihub

Lee, A. K. C., Wallace, M. T., Coo, A. B., Popper, A. N., & Fay, R. R. (2019). *Springer Handbook of Auditory Research Multisensory Processes The Auditory Perspective*. Retrieved from http://www.springer.com/series/2506

Logan, D., Kiemel, T., & Jeka, J. J. (2014). Asymmetric Sensory Reweighting in Human Upright Stance. *PLoS ONE*, *9*(6), 100418. Retrieved from www.plosone.org doi: 10.1371/journal.pone

Mackinnon, C. D. (2018). Sensorimotor anatomy of gait, balance, and falls. In *Handbook of clinical neurology* (Vol. 159, pp. 3–26). Retrieved from https://doi.org/10.1016/B978-0-444-63916-5.00001-X doi: 10.1016/B978-0-444-63916-5.00001-X

Mugge, W., Schuurmans, J., Schouten, A. C., & Van Der Helm, F. C. T. (2009). Sensory Weighting of Force and Position Feedback in Human Motor Control Tasks. *The Journal of neuroscience: the official journal of the Society for Neuroscience*, *29*(17), 5476–5482. Retrieved from https://pubmed.ncbi.nlm.nih.gov/19403815/ doi: 10.1523/JNEUROSCI.0116-09.2009

Pasma, J. H., Boonstra, T. A., Campfens, S. F., Schouten, A. C., & Van der Kooij, H. (2012, 8). Sensory reweighting of proprioceptive information of the left and right leg during human balance control. *Journal of Neurophysiology*, *108*(4), 1138–1148. Retrieved from https://journals.physiology.org/doi/10.1152/jn.01008.2011 doi: 10.1152/JN.01008.2011/ASSET/IMAGES/LARGE/Z9K0151214980010.JPEG

Proske, U., & Gandevia, S. C. (2012). The Proprioceptive Senses: Their Roles in Signaling Body Shape, Body Position and Movement, and Muscle Force. *Physiological reviews*, *92*(4), 1651–1697. Retrieved from www.prv.org doi: 10.1152/physrev.00048.2011.-This

Rosenbaum, D. A. (2009). *Human Motor Control* (2nd ed.). Elsevier Inc. Retrieved from http://www.sciencedirect.com:5070/book/9780123742261/human-motor-control doi: 10.1016/B978-0-12-374226-1.X0001-0

Saidi, M., Towhidkhah, F., Lagzi, F., & Gharibzadeh, S. (2012, 12). The effect of proprioceptive training on multisensory perception under visual uncertainty. *Journal of integrative neuroscience*, *11*(4), 401–415. Retrieved from https://pubmed.ncbi.nlm.nih.gov/23351049/ doi: 10.1142/S0219635212500276

Salmond, L. H., Davidson, A. D., & Charles, S. K. (2017). Proximal-distal differences in movement smoothness reflect differences in biomechanics. *Journal of neurophysiology*, *117*(3), 1239–1257. Retrieved from www.jn.org doi: 10.1152/jn.00712.2015.-Smoothness

Sullivan, G. M., & Feinn, R. (2012, 9). Using Effect Size-or Why the P Value Is Not Enough. *Journal of Graduate Medical Education*, *4*(3), 279–282. Retrieved from http://dx.doi.org/10.4300/JGME-D-12-00156.1 doi: 10.4300/JGME-D-12-00156.1

Van Beek, F. E., Wouter, , Bergmann Tiest, M., Kappers, A. M. L., & Gabriel Baud-Bovy, (2016). Integrating force and position: testing model predictions. *Exp Brain Res*, *234*, 3367–3379. doi: 10.1007/s00221-016-4734-1

Van der Linde, R., Lammertse, P., Frederiksen, E., & Ruiter, B. (2002). The HapticMaster, a new high-performance haptic interface. *Proc. Eurohaptics*, 1–5.

Zwerus, E. L., Willigenburg, N. W., Scholtes, V. A., Somford, M. P., Eygendaal, D., & Van Den Bekerom, M. P. (2019). Normative values and affecting factors for the elbow range of motion. *Shoulder & Elbow*, *11*(3), 215–224. doi: 10.1177/1758573217728711

Appendix A: Handle Design

A new handle is designed and fabricated to mount on the HapticMaster. The end effector of the HapticMaster is adjustable as the force sensor is located after the attachment point of the handle bar. Exchanging the end effector does not change the working principles or quality of the HapticMaster.

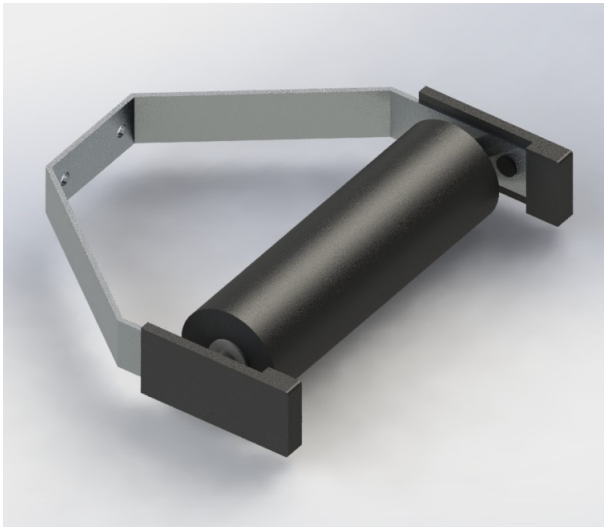

Figure 8. The handle is securely mounted onto the Haptic Master system to facilitate smooth and effortless maneuvering for the participants. This ergonomic design ensures that users can comfortably interact with the Haptic Master during the experiments. The handle incorporates two sliding bearings between the handle and the bar, effectively preventing rotation in the participants' hands. These sliding bearings guarantee a stable and fixed handle position throughout the operation, significantly improving the overall user experience and control during the experiments. Moreover, this design feature eliminates any feedback concerning how much the handle has rolled in the participants' hand palms. The frame is made of aluminium and the handle bar is made of PLA (3D printed).

Appendix B: Custom Made Elbow Brace

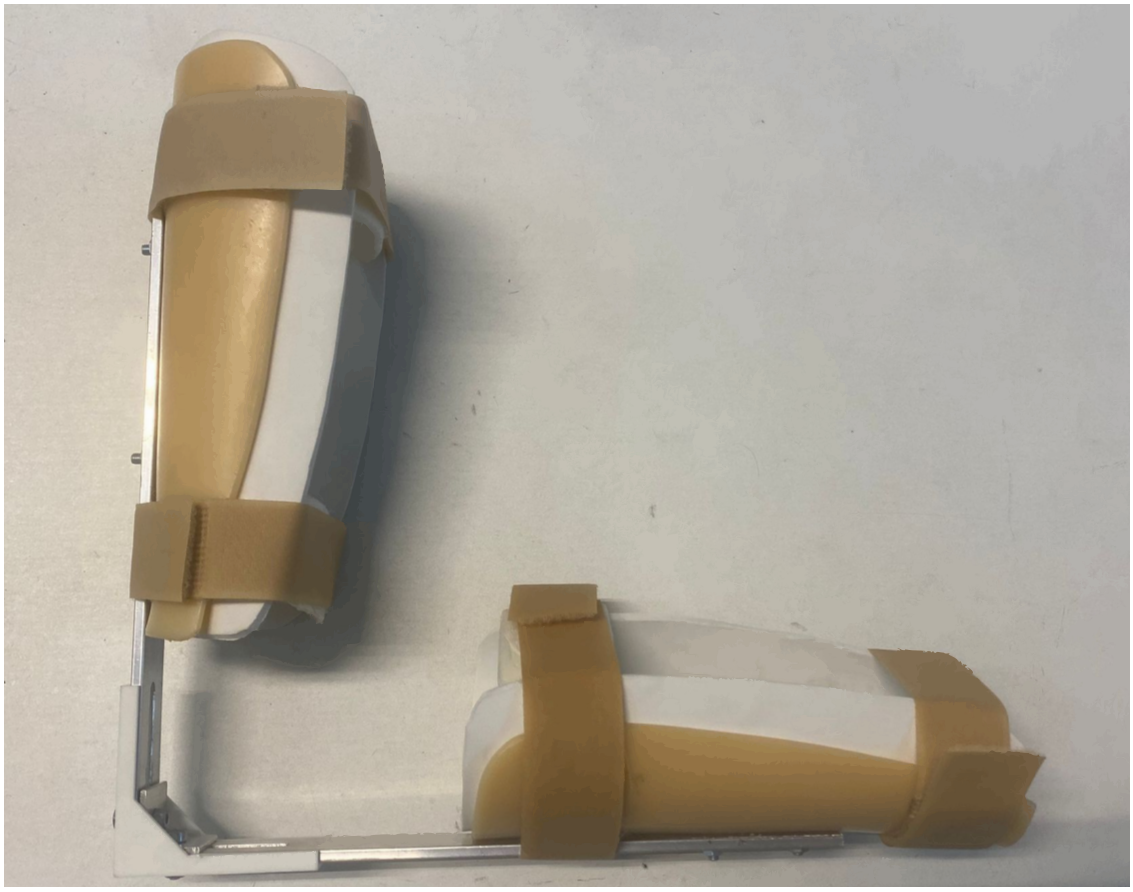

Figure 9. This brace is designed to secure both the upper and lower arms of the wearer. Its primary objective is to prevent any flexion of the elbow joint. The position of both the upper and lower arm components of this brace is adjustable, allowing it to accommodate all participants comfortably. A 3D printed corner is added to strengthen the brace.

Appendix C: Participant Information

Participant	Age	Handedness	Gender	Height [m]	Arm Segment Lengths [m]:		
					Wrist	Elbow	Shoulder
1	24	Right	Female	1.60	0.0550	0.2830	0.3750
2	23	Right	Female	1.72	0.0600	0.2900	0.3950
3	24	Right	Female	1.62	0.0600	0.2700	0.4300
4	23	Right	Female	1.71	0.0570	0.3020	0.4500
5	23	Left	Female	1.65	0.0580	0.2600	0.3950
6	24	Right	Female	1.69	0.0530	0.2080	0.3950
7	24	Right	Female	1.69	0.0530	0.2940	0.4250
8	24	Right	Female	1.76	0.0570	0.3160	0.456
9	22	Right	Female	1.60	0.0540	0.2640	0.3700
10	21	Right	Female	1.74	0.0560	0.2940	0.4250

Table 6. Participant information

Appendix D: Calculation of Joint Angles

Table 7. Calculation of the joint angles (θ) based on the coordinates of the HapticMaster (HM) in two dimensions (x,z).

Definition	Formula
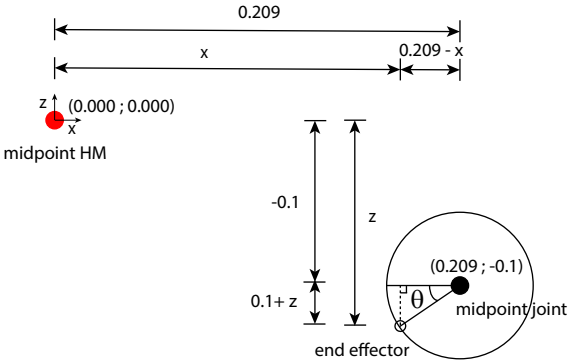	$\theta_{wrist} = acos(\frac{(0.1+z)}{\sqrt{(0.1+z)^2+(0.209-x)^2}})$
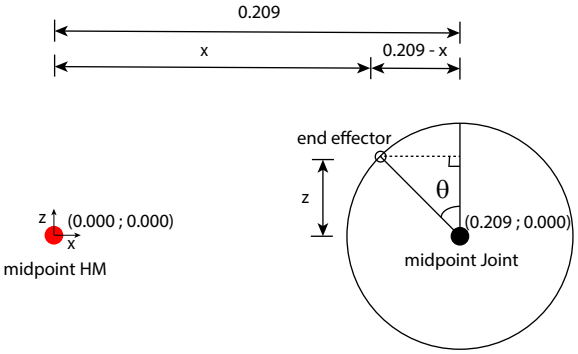	$\theta_{elbow} = acos(\frac{z}{\sqrt{z^2+(0.209-x)^2}})$
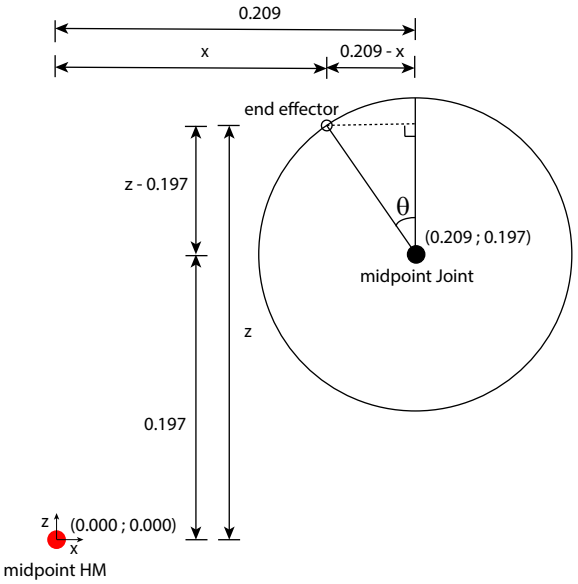	$\theta_{shoulder} = acos(\frac{z-0.197}{\sqrt{(z-0.197)^2+(0.209-x)^2}})$

Appendix E: Validation of AtiDaq 45 Mini Force Sensor

The ATIDAQ mini 45 force sensor is employed for the experiments. To ensure its accuracy, two weights of 750 grams and 1000 grams are utilized. These weights are positioned in the middle of the layered handle, as participants will place their hand at this location. The weights are oriented in the positive X direction, so the force sensor (XForce) should register a reading equal to the gravitational force exerted by the weight. The output of the force sensor is measured in voltage units. These voltage measurements are then used to calculate the corresponding forces and torques. The purpose of this experiment is to validate both the sensor's performance and the accuracy of the calculations. Each weight is subjected to four trials, with each trial consisting of six measurements. Before commencing each trial, the force sensor is calibrated, and between each measurement, the weight is removed from the handle to ensure accuracy. The results of the measurements for the experiments with the 750-gram weight are recorded in Table 8, while the trials with the 1000-gram weight are documented in Table 9.

$$F = 0.7500 * 9.8100 = 7.3575N$$

trial 1	trial 2	trial 3	trial 4
7.3589	7.2241	7.2928	7.3965
7.3986	7.2429	7.1961	7.3894
7.3620	7.2546	7.2785	7.3274
7.3309	7.2190	7.4001	7.3253
7.3238	7.2348	7.2556	7.3518
7.3518	7.1875	7.2643	7.4077
7.3543	**7.2272**	**7.2812**	**7.3664**

Table 8. Experiment with a load of 750 grams loaded to the force sensor to validate the functioning of the force sensor and test the calculation from voltage to force.

$$F = 1.000 * 9.8100 = 9.8100N$$

trial 1	trial 2	trial 3	trial 4
9.7542	9.8621	9.8931	9.8158
9.8605	9.8504	9.8280	9.8229
9.9124	9.8748	9.8738	9.7395
9.9114	9.7888	9.8341	9.7964
9.8987	9.9485	9.9272	9.8661
9.8397	9.9099	9.8895	9.8346
9.8628	**9.8724**	**9.8743**	**9.8126**

Table 9. Experiment with a load of 1000 grams loaded to the force sensor to validate the functioning of the force sensor and test the calculation from voltage to force.

Appendix F: Maximum Likelihood Estimation

Within the MLE model, the weighting factors are calculated based on the variance of each cue. Within both equations, s_f represents the standard deviation of the force task and s_x the standard deviation of the position task.

$$W_x = \frac{\frac{1}{k^2 * s_x^2}}{\frac{1}{s_f^2} + \frac{1}{k^2 * s_x^2}}$$

$$W_f = \frac{\frac{1}{s_f^2}}{\frac{1}{s_f^2} + \frac{1}{k^2 * s_x^2}}$$

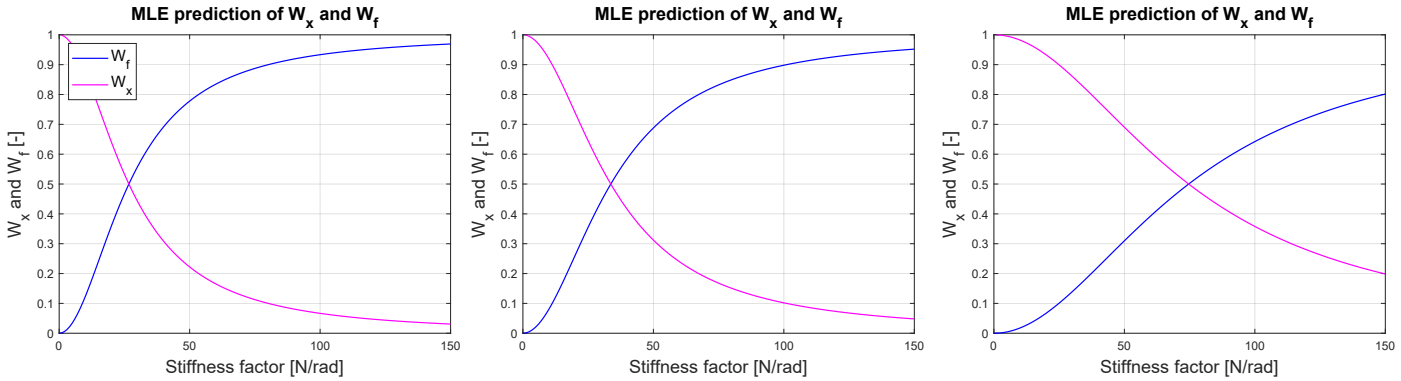

a Wrist **b** Elbow **c** Shoulder

Figure 10. MLE model based on participant 1

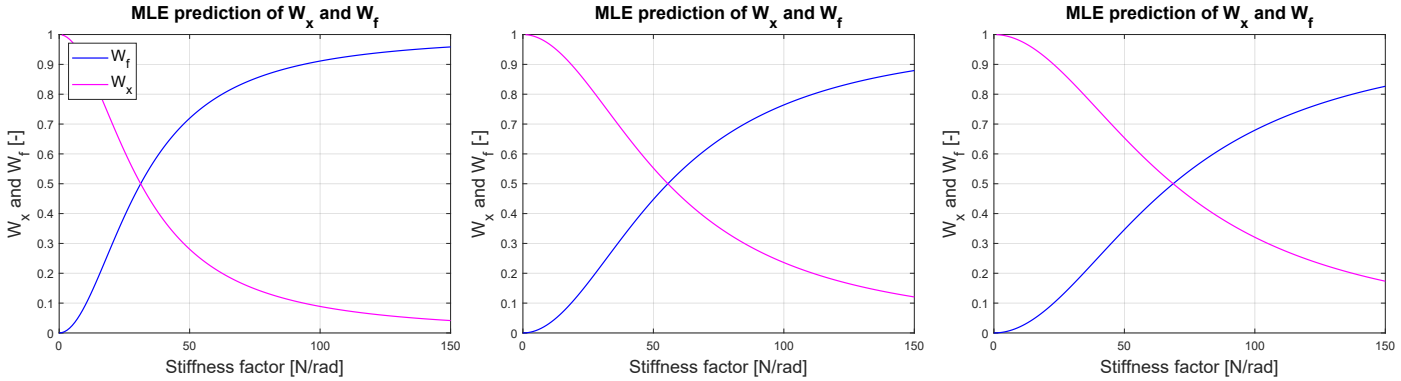

a Wrist **b** Elbow **c** Shoulder

Figure 11. MLE model based on participant 2

Appendix G: Data Exclusions

Data exclusions occur after the complete storage of all data. These exclusions arise in response to disruptions encountered during the trials. These disruptions primarily encompass instances where participants either failed to maintain the end effector at the designated target locations before clicking, instead moving before the click, or instances where participants inadvertently performed a double-click at the beforehand target while situated at the target location, so that this next target is not representative. Per participant, a total of 720 data points is collected. For all participants, lower than 2.5 % of the data points collected is considered as failed trial and therefore deleted. The exclusions are included in Table 10. For the exclusions, the first word refers to the joints, and the second word to the type of trial. The first number refers to the stiffness condition, the second number to the number of trial (1 out of 10), and the third number (in the brackets), refers to which number of that type of trial. So for example, wrist: blind-50-2(2) refers to the blind trial for the wrist, in stiffness condition, k = 50 N/rad. It is the second trial and within this trial, the second blind trial.

$$3 \text{ (stiffness conditions)} \cdot 10 \text{ (trials)} \cdot 8 \text{ (targets)} \cdot 3 \text{ (joints)} = 720 \text{ data points}$$

Participant	Exclusions: Wrist	Elbow	Shoulder	Total percentage of exclusion
1	blind-50-2(2) blind-50-3(2) blind-50-4(1) blind-50-7(1) catch-50-9(2) blind-50-10(1)	catch-80-1(2) catch-80-2(2) catch-80-7(2)	blind-15-1(1) blind-15-5(2) blind-50-5(2) blind-50-7(1) blind-50-10(1) blind-50-10(2) blind-80-3(2) blind-80-6(2) blind-80-9(2)	2.5 %
2	blind-80-2(2)		blind-50-7(2)	0.28 %
3	catch-80-8(2) blind-80-9(2)	blind-15-6(2) blind-80-3(1) catch-80-4(2) blind-80-10(2)	blind-15-3(2) blind-80-7(2)	1.11 %
4		catch-80-2(1) catch-80-3(1) catch-80-7(2) blind-80-8(2) blind-80-9(2)		0.69 %
5		catch-80-8(2) catch-50-10(2) catch-80-7(2) blind-80-8(2) blind-80-9(2) blind-80-10(2)		0.83 %
6	blind-15-5(2) catch-15-10(2) blind-50-10(2)	blind-50-6(2) blind-80-1(1)		0.69 %
7	catch-15-6(1) blind-80-5(1) catch-80-9(2)	catch-15-2(2) catch-15-8(2)	catch-15-6(2) catch-15-10(1) catch-50-3(1)	1.11 %
8	catch-15-4(1) blind-15-7(1) blind-80-1(1)	catch-80-5(2)	catch-50-7(2) catch-50-10(1)	0.83 %
9	catch-15-3(2) blind-80-1(2) catch-80-3(2) blind-80-10(1)	blind-50-3(2)		0.69 %
10	blind-15-2(2) catch-15-10(1) blind-50-6(1) catch-50-6(2) catch-80-8(2)	blind-15-4(1) catch-15-9(1) blind-15-1(1) blind-15-1(2) catch-15-1(1) catch-15-1(2) catch-50-2(2) blind-50-10(2) catch-80-6(1) catch-80-6(2)	blind-15-4(2) blind-15-7(2) blind-80-8(2)	2.5 %

Table 10. Data point exclusions.